EXPERIMENTAL STUDY OF AIRCRAFT STABILITY ENHANCEMENT AT HIGH ANGLES OF ATTACK

A. Huang*
Wackett Aerospace Centre RMIT
GPO Box 2476V
Melbourne Vic. 3001
AUSTRALIA

Abstract

An investigation on the effectiveness of ventral fins in controlling aircraft lateral/directional stability at high angles of attack was carried out in the Aero Industry Development Center low speed wind tunnel in Taiwan, ROC. The baseline model, a modified design from NASA TP-1803 report, with single ventral-fin attachment was used in the testing. Ventral fins employed included a rectangular, a trapezoidal and a triangular shape, with the same surface area, thickness and interface length, but different aspect ratio. It was found that the effectiveness of ventral fins in controlling lateral/directional stability was dominated by the ventral fin aspect ratio and ventral fin attachment location. By working similarly with the vertical tail, ventral fins located behind the aircraft moment center increased directional stability but decreased lateral stability. The triangular ventral fin was found the most effective shape among the three towards directional stability enhancement. Due to boundary layer consideration, the greater aspect ratio the ventral fin has, the more effective the ventral fin is in controlling directional stability. However, side effects on lateral stability increase as the aspect ratio becomes larger. Ventral fins located in front of the aircraft moment center were found to decrease both lateral and directional stability.

Nomenclature

C_L	lift coefficient
C_l	rolling moment coefficient (body axis system)
$C_{l\beta}$	lateral stability ($dC_l/d\beta$)
C_{ls}	rolling moment coefficient (stability axis system)
C_m	pitch moment coefficient
C_n	yawing moment coefficient (body axis system)
$C_{n\beta}$	directional stability ($dC_n/d\beta$)
C_{ns}	yawing moment coefficient (stability axis system)
α	angle of attack (deg)
β	sideslip angle (deg)

Abbreviations

AIDC	Aero Industry Development Center, Taiwan
AOA	angle of attack
ARL	Aeronautical Research Laboratory, AIDC
MC	moment center
VF	ventral fin

1. Introduction

Aircraft maneuverability is extremely important in combat aircraft design. In order to achieve this, it is necessary for aircraft to fly at high angles of attack (AOAs)[1, 2, 3, 4]. For aircraft to manoeuvre effectively in the low speed, high AOA flight regime, a high level of control effectiveness about longitudinal, lateral and normal axes is required. However, aircraft tend to become unstable in this flight regime. With increasing AOA, the airflow is no longer able to be attached to the body surface, and it starts to separate. As the flow separates and forms wake near aircraft stability or control surfaces, such as the vertical tail and rudder, the effectiveness of these stability and control devices is seriously degraded.

At low AOAs the vertical tail provides significant contribution to directional stability. In asymmetric flight with a sideslip angle the vertical tail acts as a wing surface and induces a side force. Because of its moment arm about the aircraft's center of gravity, it generates a yawing moment which tries to reduce the sideslip angle and thus has a stabilizing effect. The larger the surface of the vertical tail, the greater the resultant force is acting on the stability surface, and hence the greater the effect is produced. However, due to aeroelastic considerations the vertical tail span cannot be too large. Thus as the angle of attack is increased, the limited size of vertical tail is

* Undergraduate student

gradually immersed in the wake of the fuselage and the wing, and its effectiveness falls off.

An exceptionally useful method in controlling the directional stability of an aircraft, particularly at high AOAs, is by attaching ventral fins(VFs). VFs are expected to work in the similar way as the vertical tail, except that they are believed to perform better in the higher AOA range[1]. The attachment of VFs has been verified to be more effective than enlarging the vertical tail surface because of the favourable interference behaviour between VFs and the fuselage. However, the relatively small size of VFs makes them more or less ineffective at low AOAs, particularly if they lie in the flow aft of externally carried loads under the fuselage and are in the relatively thick fuselage boundary layer.

The objective of this paper is to investigate the effectiveness of VFs in controlling lateral/directional stability at high AOAs.

2. Experimental Details

2.1 Test Facility and Model Description

The tests were performed in the AIDC low speed wind tunnel with a 7-ft by 10-ft test section. The velocity range of the tunnel can be varied from 10 mph to 220 mph. The maximum allowable Reynolds number is 2.0×10^6 /ft.

The model support system consists of a sting and an automated pitch and yaw mechanism which are remotely manipulated by a digital control panel. The sting supports models through their rear hollow sections. This design minimizes the influence of the support to the airflow. In order to have both low and high AOA test range, 2 sets of supporting systems were used. The 26° offset sting is used for lower AOA tests, and the angle can range from -6° to 26°. The angle is controlled by adjusting the ram height and pitch head angle. The 45° offset sting is used for higher AOA tests, and the angle range is between 10° and 38°. The sideslip angle for both stings can be varied between ± 20°.

The model forces and moments are measured by ABLE MK-XXVIII internal balance(six component strain gauge type). The data is collected by ANDS 5400 data acquisition system and is further processed by PDP 11/23 computer.

The test involved testing six different VFs in three different shapes in conjunction with a baseline model, as shown in **Fig. 1**. Single fin attachment was employed in the test. The baseline configuration was a modified design from NASA TP-1803 report. Its forward body was redesigned to become a tangent ogive with a fineness ratio of 3.14, and the model size was increased by 1.6 times. The aspect ratio and taper ratio of the baseline wings were 2.5 and 0.2 respectively. VFs employed included a rectangular, a trapezoidal, and a triangular shape, with two fins in each shape for either front or rear attachment to the fuselage bottom surface. They were located with a horizontal distance of 20-in between their centroids and the baseline moment centre. Each fin had the same surface area(30 in^2), thickness(0.125 in) and interface length (7.5 in), but different aspect ratio. The VF area was about half the size of the vertical tail. The fins were sharpened at edges.

2.2 Test Conditions and Procedure

Seven configurations of models were involved in the tests, including the baseline without VFs to which comparisons can be made and the baseline with six sets of VFs with three different shapes for two different attachment locations.

The tests were basically measuring forces and moments at different α and β. The reference location for measurements was at the aircraft MC, as shown in **Fig. 1**. The operating velocity of the airflow was fixed at a Mach number of 0.17 with the Reynolds number of 1.3×10^6. The test α ranged from -3° to 38° with an interval of 2° ~ 5°, and β was varies between ±10° with an interval of 1° ~ 2°.

3. Results and Discussion

The experimental results are subdivided into stability analysis in longitudinal direction and lateral direction which includes yaw and roll modes.

3.1 Longitudinal Stability

The longitudinal performance of the baseline configuration is shown as the relations between C_L, C_m and α in **Fig. 2**. As shown in the lift-curve slope(**Fig. 2a**), there is no lift at zero incidence for uncambered aerofoils. The curve is kept straight up to $\alpha \approx 10°$, and this straight section represents that airflow follows the aircraft surface and no separation occurs. At $\alpha = 12°$, flow starts to separate at the trailing edge of the wing. The airflow fully separates from the wing at $\alpha = 18°$ with $C_L = 0.81$. The $C_{Lmax} = 0.92$ occurs at $\alpha = 28°$. The further extension of lift curve after $\alpha = 18°$ is due to the vortex lift increase of the forward body. As **Fig. 2b** shows, the pitching moment decreases until $\alpha = 28°$. Since the stable condition in the longitudinal direction implies the $dC_m/dC_L < 0$, the baseline is longitudinally stable up to $\alpha = 18°$, since C_m vs C_L curve slope becomes negative at $\alpha = 18°$, as illustrated in **Fig. 2c**.

The comparison between the baseline and baseline with rear VFs is shown in **Fig. 3**. The superimposed curves for all configurations indicate that VFs located at the rear do not affect aircraft longitudinal performance at all. However, when VF attachment location is considered, as shown in **Fig. 4**, there is a slight difference between the two cases. Since all shapes of VFs show the same pattern of phenomenon, only the curves for triangular VFs are shown here. For the baseline with triangular VF attached at the front, the C_L are higher than these of other cases at $\alpha = 18^\circ \sim 26^\circ$. The VF located at the front seems to have little influence on aircraft longitudinal behaviour. The triangular VF at the front improves vortex symmetry at the forward body and increases vortex lift and hence C_L.

3.2 Lateral/Directional Stability

The aircraft coordinate system is defined by either the body axis or stability axis system. In the present study, in addition to the body axis system, the stability system is also used to determine lateral/directional stability. When the stability axis system is employed, yawing and rolling moment coefficients are defined by:

$$C_{ns} = C_n\cos\alpha - C_l\sin\alpha$$
$$C_{ls} = C_l\cos\alpha + C_n\sin\alpha$$

3.2.1 Vortex Asymmetry

The yawing and rolling moment coefficients of the baseline at zero sideslip angle are shown as a function of AOA in **Fig. 5**. As the figure shows, the baseline is directionally and laterally stable until $\alpha = 20^\circ$. At $\alpha = 20^\circ$, a limited amount of vortex asymmetry starts to occur and induces slight yawing and rolling moments. At $\alpha = 25^\circ$, yawing and rolling moments change their signs(direction) because of the alternation of the vortex arrangement. The phenomenon of vortex asymmetry becomes obvious above this AOA.

As illustrated in **Fig. 6**, C_n vs α and C_l vs α curves for VFs attached at the rear closely match the one for the baseline in both pattern and magnitude. The only tiny changes are the appearance of slight yawing moments at lower AOAs and slight magnitude reduction of rolling moment for the baseline with rear VFs. However, by comparing curves for the forward and rear VFs as shown in **Fig. 7**, it is obvious that the VF at the front induces lower magnitude of yawing moment at zero sideslip than the VF at the rear does throughout all AOA. So it can be concluded that generally VFs at the rear do not have effects on vortex asymmetry, but the forward VFs do.

3.2.2 Directional Stability(Yawing)

For the purpose of replacing the function of the vertical tail at high AOAs, the effectiveness of VFs in controlling aircraft directional stability should be the first point to be considered. Their side effects on rolling is not as important as their effects on yawing, since lateral(rolling) stability can be controlled by other devices.

By referring to **Fig. 8**, it can be seen that the baseline becomes directionally unstable above a certain AOA(20°), and the unstable condition is more likely to occur at large sideslip angles. The C_n vs β curves for body axis and stability axis systems are quite similar.

As illustrated in **Fig. 9**, it is obvious that rear VFs improve directional stability greatly throughout all range of AOAs. As sideslip angle increases, a side force tends to be induced acting on the VF and pushes the fin back to the direction of the freestream if the fin is located behind the aircraft MC. All rear VFs extend the directional stable condition from $\alpha = 28^\circ$ for the baseline model to $\alpha = 38^\circ$, which is the test limit.

Experimental results show that the triangular VF located at the rear is the most effective fin in controlling directional stability. The trapezoidal fin comes second, and the rectangular fin comes third. The aspect ratio is 0.533 for the rectangular fin, 0.833 for the trapezoidal fin, and 2.133 for the triangular fin. By looking at the dimensions of each VF carefully, it would be more reasonable and appropriate to conclude that stabilizing effect of VFs depends on the aspect ratio or span of the fin rather on the shape of the fin. By considering the boundary layer effect, flow speed reduces near the body surface in viscous airflow. Therefore the higher the aspect ratio of the VF, the longer span the fin extends downwards, and the greater the area of the fin is in the free stream. Hence the greater the resultant force is acting on the VF.

As **Fig. 9(b)** shows, the triangular VF in front of MC lowers yawing stability throughout all α and reduces directional stable condition limit from $\alpha = 28^\circ$ to $\alpha = 15^\circ \sim 20^\circ$. As there is a sideslip angle, the yawing moment induced rotates the aircraft further away from the freestream direction and increases the sideslip angle.

3.2.3 Lateral Stability(Rolling)

As shown in **Fig. 10**, the baseline lateral stability performance is slightly different by using two different axis systems. By using the body axis system, the baseline becomes unstable at $\alpha = 28^\circ$. The stability gets worse for larger β. However, when α approaches the test limit ($35^\circ \sim 38^\circ$), the stability seems to become acceptable again. On the other hand, the unstable condition occurs at $\alpha = 15^\circ$ for stability axis system. As the incidence increases, the rolling stability gets better again even though C_l is not close to zero at zero sideslip.

In **Fig. 11(a)**, it is shown that VFs lower lateral stability throughout all range of AOAs. The side force and the

distance in normal(vertical) direction between the fin centroid and the aircraft MC generate an unstable rolling moment. As shown in **Fig. 11(b)**, the triangular VF at the front performs better in rolling stability than the one at the back does at AOAs up to 15°. From this angle to $\alpha = 20°$ the VFs at both locations have similar performance — the aircraft becomes unstable. At $\alpha > 20°$, stability improves and the rear triangular VF generates less side effects to rolling stability than the front one does.

3.3 Ventral Fin Effectiveness

Generally VFs have no effect on longitudinal stability. They improve directional stability, but decrease lateral stability. They can never be located in front of the aircraft MC.

Since stability is defined by unit change of moment per unit change of β, and a moment is composed of a force and a moment arm, aircraft stability depends basically on the magnitude of the force and the length of the moment arm. The magnitude of the resultant force acting on the VF depends on size of the effective surface area or aspect ratio of the VF, and the moment arm depends on the aircraft MC location and the VF centroid location. Therefore basically the larger the size of these variables, the greater magnitude of a moment is produced. However, due to ground clearance limit and aeroelastic considerations, VFs cannot be too large.

By solely considering the directional stability, the surface area and aspect ratio of the VF and the longitudinal distance between the aircraft MC and the fin centroid have to be kept as large as possible with considerations of various limits. On the other hand, by considering lateral stability solely, the VF area and VF span must be kept small in order to minimize rolling. Thus when designing VF, negotiation will need to be made between the two aspects. However, as the objective of the use of VFs is to enhance the function of the vertical tail, lateral stability is not as critical as directional one.

4. Conclusions and Recommendations

Experimental results show that the effectiveness of VFs in controlling lateral/directional stability is dominated by the VF aspect ratio(shape) and VF installation location. The investigation of VFs through testing leads to the following conclusions:

1. A single VF located behind aircraft MC does not influence aircraft longitudinal stability.
2. A single VF located behind aircraft MC improves directional stability greatly throughout all range of AOAs.
3. A single VF located behind aircraft MC with higher aspect ratio is better in controlling directional stability but worse for lateral stability.
4. A single VF can never to installed in front of aircraft MC.
   - It lowers both lateral and directional stability throughout all AOAs.
   - They reduce range of AOAs allowed for stable flight.

In this investigation, the triangular VF installed behind the baseline MC is the best configuration among all, which fulfills the objective of the use of single VF. If the best design of VFs is to be determined, further investigations of the effects of VF area, VF centroid location in longitudinal and lateral directions, VF shape, VF aspect ratio, number of VFs attached and their inclined angle on aircraft stability will need to be conducted.

Acknowledgements

The project was supported by AIDC under the guidance of Dr. Ray C. Chang. The author would like to thank Dr. Chang for initiating the investigation and for his continuous advise and kind assistance. The author would also like to acknowledge Wackett Aerospace Centre RMIT for granting partial financial support for attending the ICAS Congress.

References

1. Huenecke, K., "Modern Combat Aircraft Design," Naval Institute, 1987.
2. Huang, J.M., "Stability Enhancement Investigations of IDF at High Angles of Attack," ARL/AIDC Paper, 1991.
3. Lan, C.E., Emdad, H., and Chin, S., "Calculation of High Angle-of-attack Aerodynamics of Fighter Configurations," AIAA-89-2188, 1989.
4. Chambers, J.R. and Grafton, S.B., "Aerodynamic Characteristics of Airplanes at High Angles of Attack," NASA Technical Memorandum 74097.

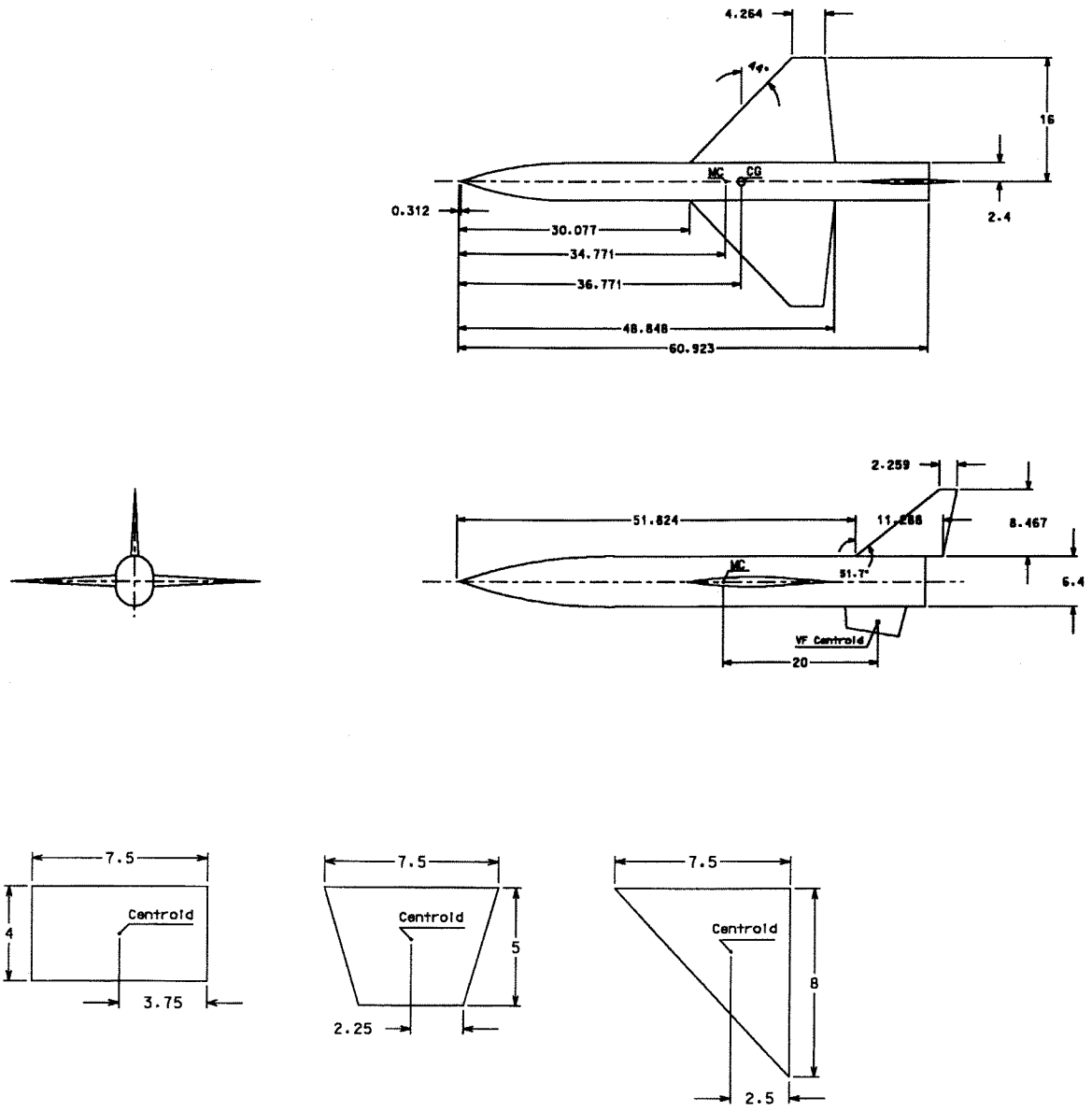

Rectangular VF
A.R. = 0.533

Trapezoidal VF
A.R. = 0.833

Triangular VF
A.R. = 2.133

Figure 1 Geometry of the test models (linear dimensions in inches)

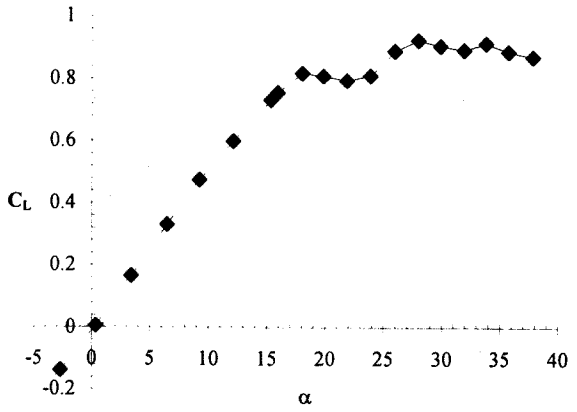

(a) C_L vs α

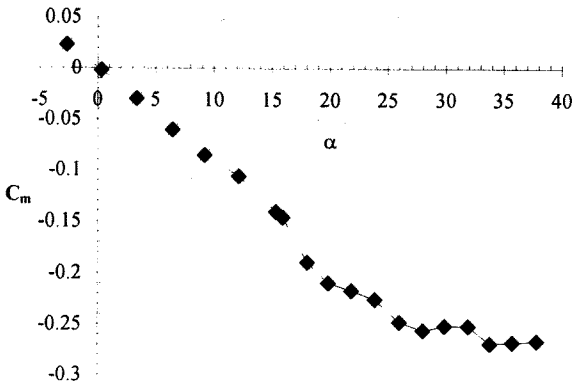

(b) C_m vs α

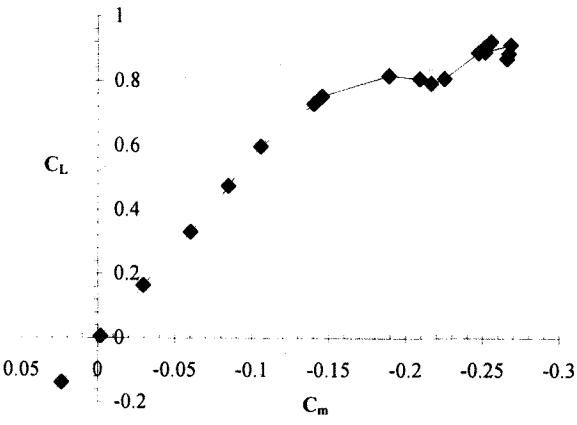

(c) C_L vs C_m

Figure 2 Longitudinal characteristics for the baseline configuration

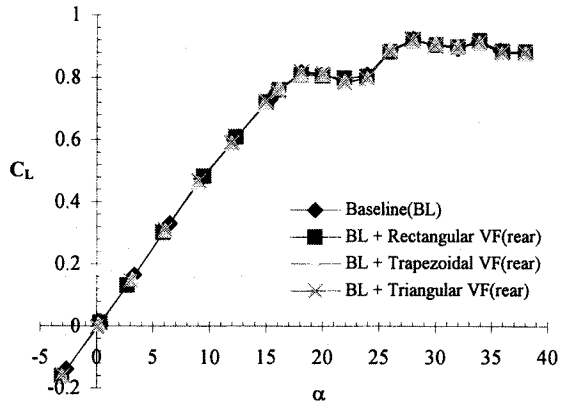

(a) C_L vs α

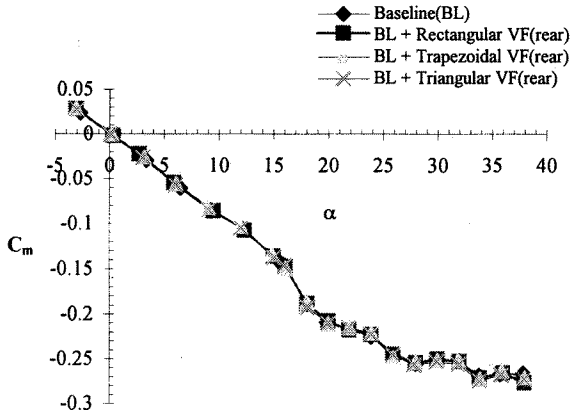

(b) C_m vs α

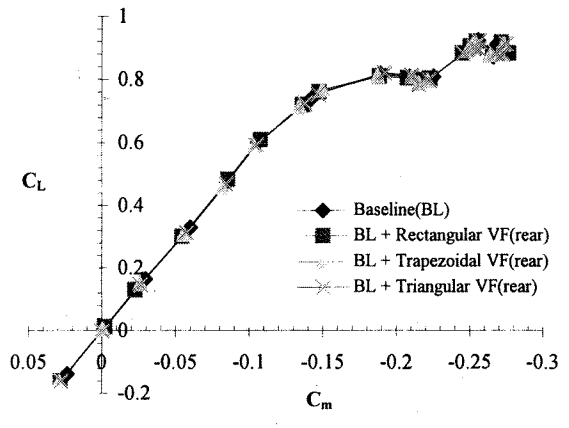

(c) C_L vs C_m

Figure 3 Longitudinal characteristics for the baseline & baseline + VF configurations

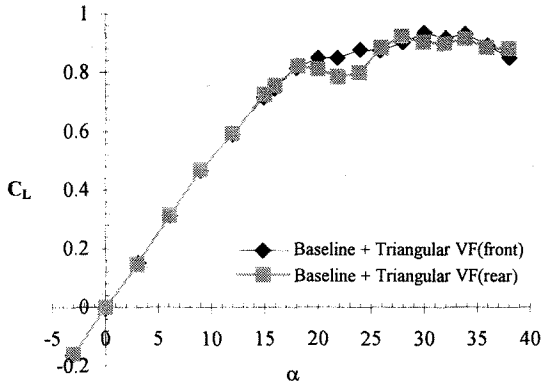

(a) C_L vs α

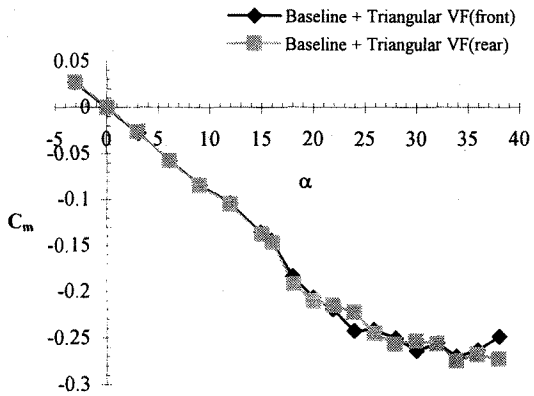

(b) C_m vs α

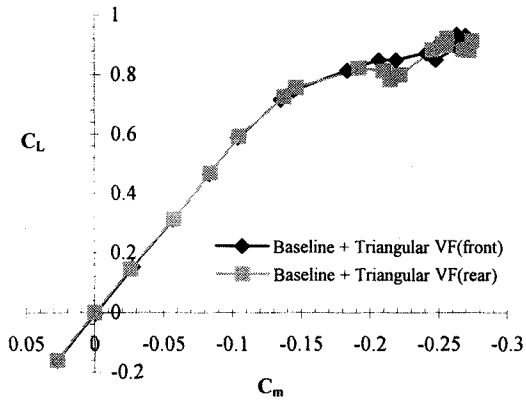

(c) C_L vs C_m

Figure 4 VF location effects on longitudinal characteristics

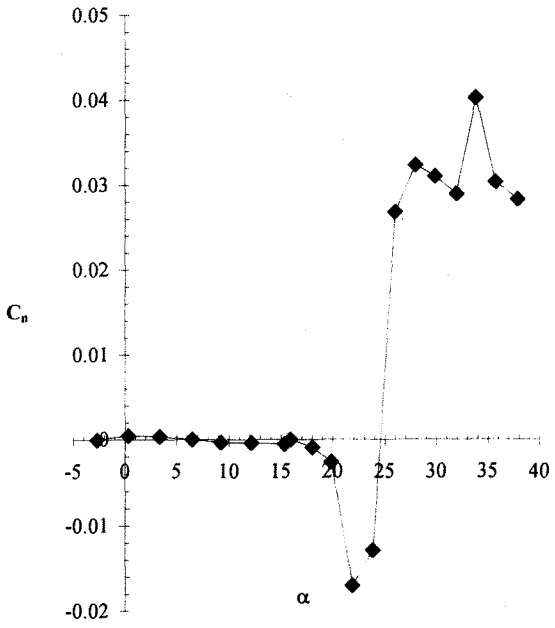

(a) C_n(body axis) vs α

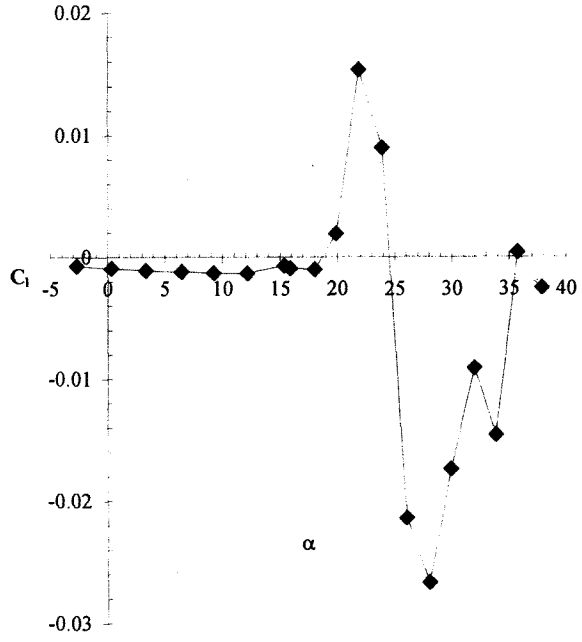

(b) C_l(body axis) vs α

Figure 5 Yawing & rolling moment coefficients for the baseline at zero sideslip

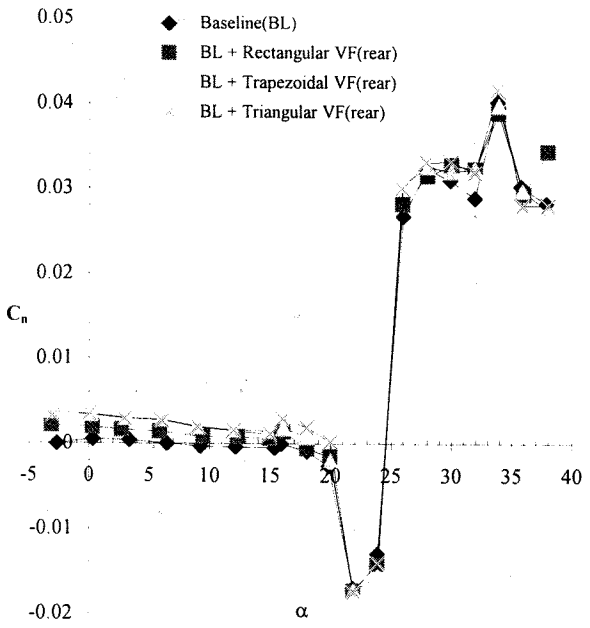

(a) C_n(body axis) vs α

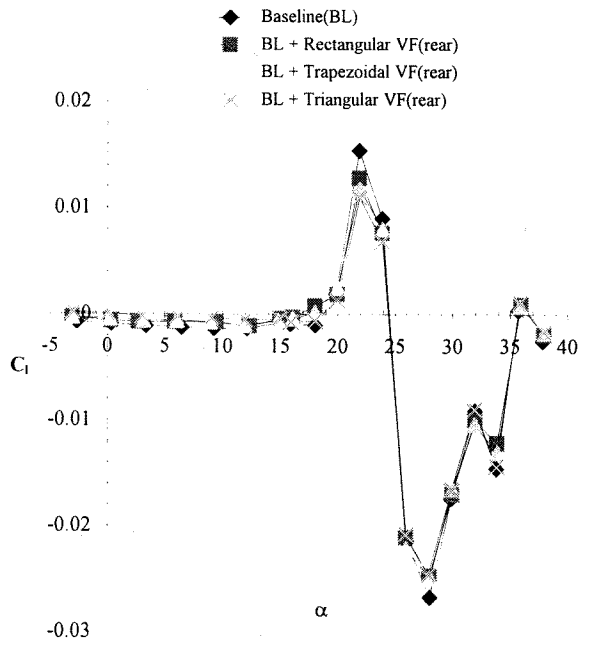

(b) C_l(body axis) vs α

Figure 6 Yawing & rolling moment coefficients for the baseline & baseline + VFs at zero sideslip

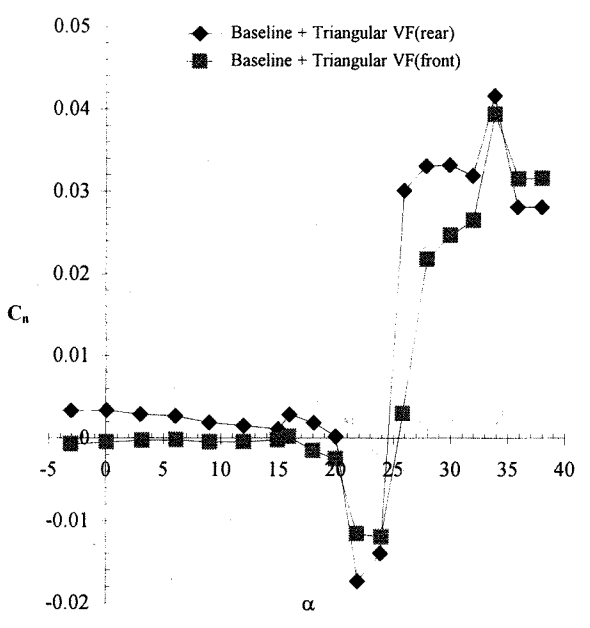

(a) C_n(body axis) vs α

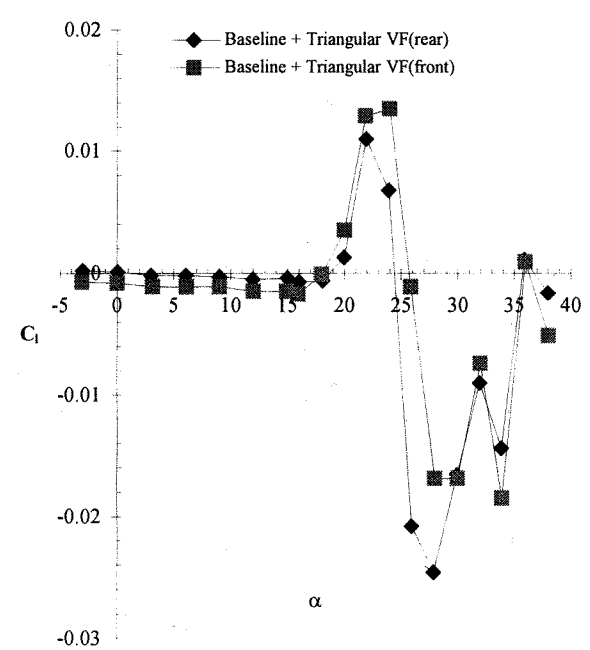

(b) C_l(body axis) vs α

Figure 7 Location effects on yawing & rolling moment characteristics at zero sideslip

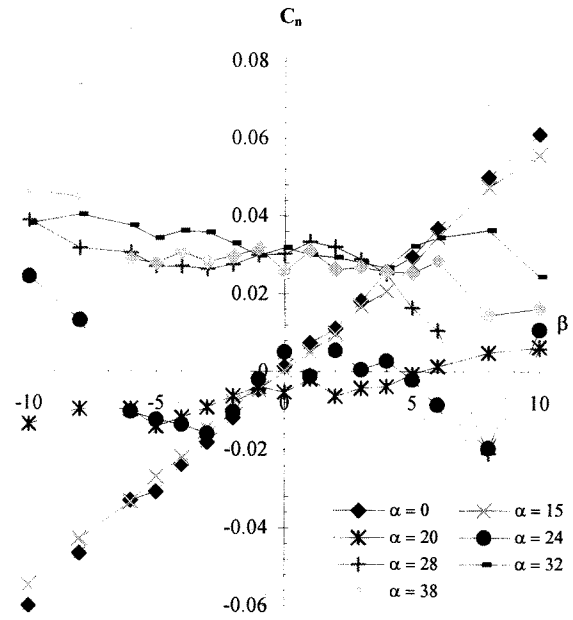

(a) C_n(body axis) vs β - BASELINE

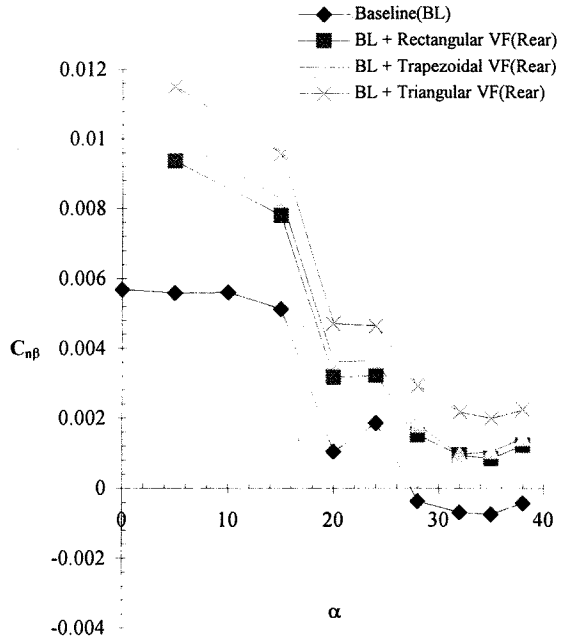

(a) $C_{n\beta}$ vs α

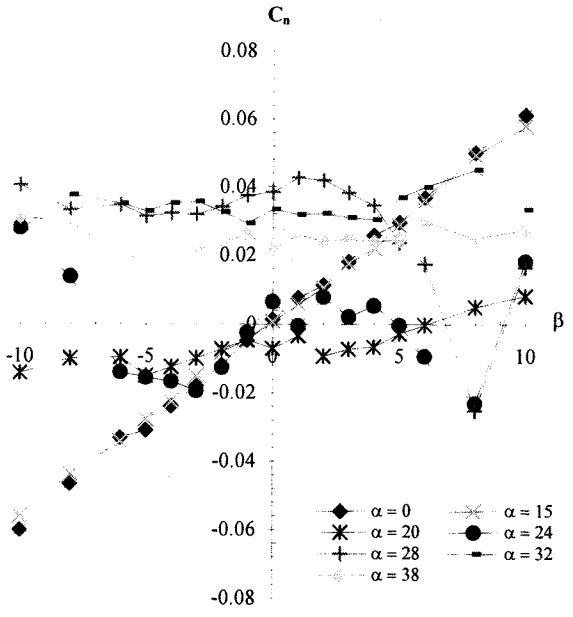

(b) C_n(stability axis) vs β - BASELINE

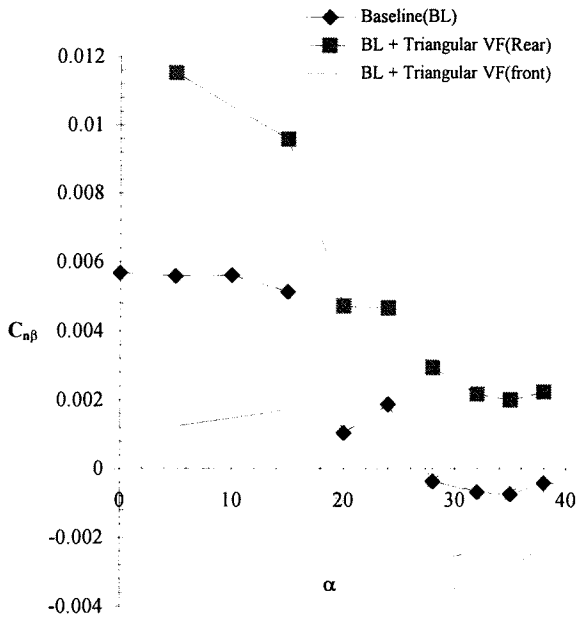

(b) $C_{n\beta}$ vs α (VF location effects)

Figure 8 Yawing moment characteristics for the baseline

Figure 9 VF effects on directional stability

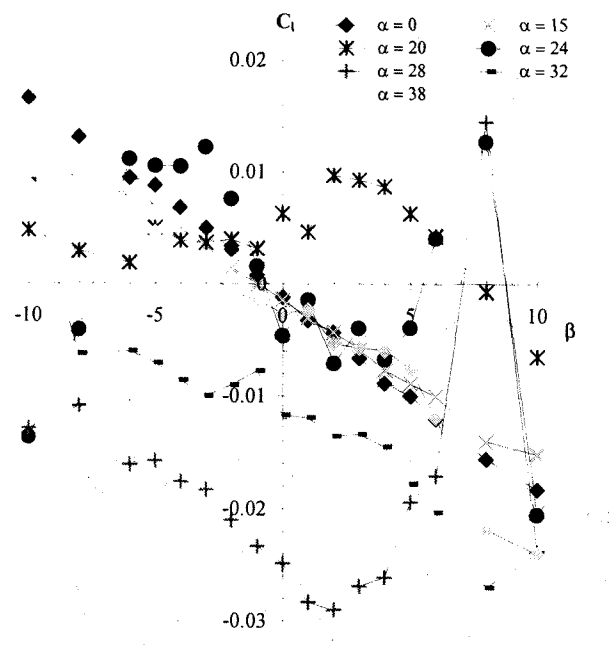

(a) C_l(body axis) vs β - BASELINE

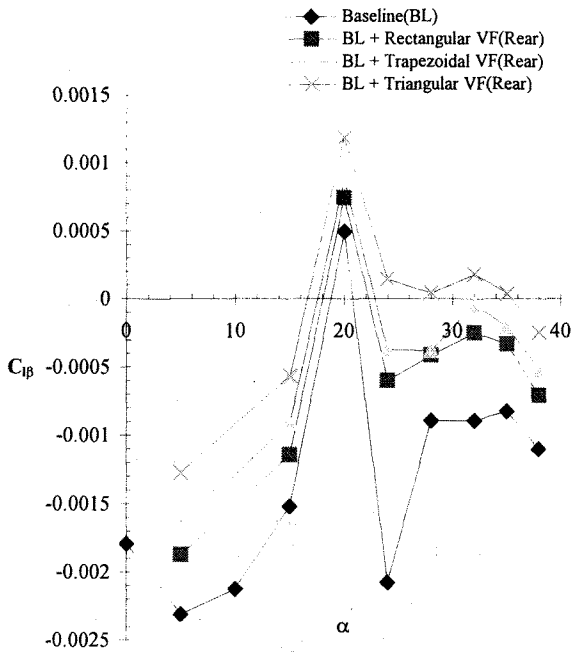

(a) $C_{l\beta}$ vs α

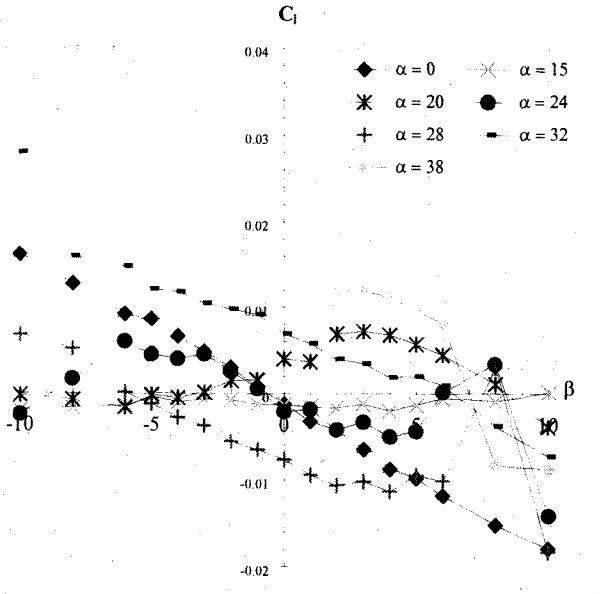

(b) C_l(stability axis) vs β - BASELINE

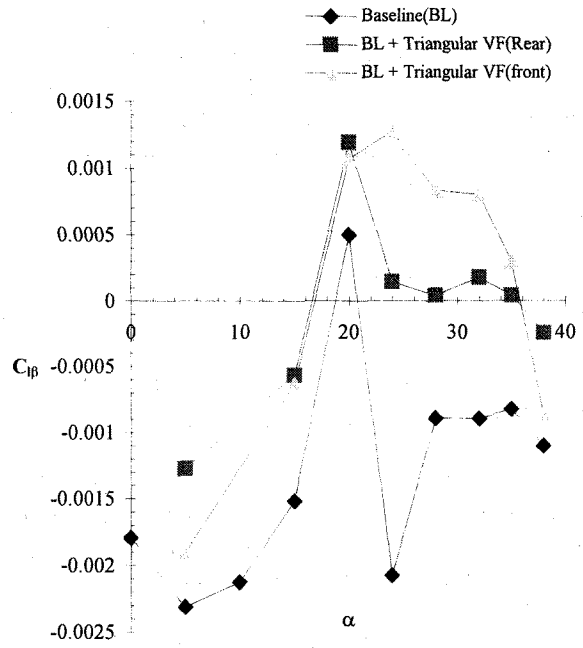

(b) $C_{l\beta}$ vs α (VF location effects)

Figure 10 Rolling moment characteristics for the baseline

Figure 11 VF effects on lateral stability